Front. Phys. 10(5), 102401 (2015)
DOI 10.1007/s11467-015-0510-0

RESEARCH ARTICLE

Nuclear dynamical octupole deformation in heavy-ion reactions

Cheng Tang[1], Xin Jin[1], Nan Wang[1,†], En-Guang Zhao[2,3,4]

[1] *College of Physics, Shenzhen University, Shenzhen 518060, China*

[2] *State Key Laboratory of Theoretical Physics, Institute of Theoretical Physics, Chinese Academy of Sciences, Beijing 100190, China*

[3] *Center of Theoretical Nuclear Physics, National Laboratory of Heavy Ion Accelerator, Lanzhou 730000, China*

[4] *School of Physics, Peking University, Beijing 100871, China*

Corresponding author. E-mail: [†] *wangnan@szu.edu.cn*

Received August 20, 2015; accepted September 22, 2015

Within the quantum molecular dynamics (QMD) model, the dynamical octupole deformation is studied as a function of the central distance between the projectile and target in the approaching process of heavy-ion fusion reactions. The dependence of the maximum dynamical octupole deformations on the incident energies is also investigated. The dynamical octupole deformations can be observed during the approaching process, and the maximum dynamical octupole deformations become more significant with decreasing incident energies. The distributions of the proton and neutron centers in the projectile and target are also investigated, respectively. In the approaching process of heavy-ion fusion reactions, the separation between proton centers for two nuclei is larger than that between neutron centers because of the strong Coulomb potential.

Keywords heavy-ion reactions, nuclear deformation, quantum molecular dynamics model

PACS numbers 24.10.-i, 25.70.Jj, 24.60.Dr, 27.90.+b

The heavy-ion reaction mechanism is an important and interesting topic in the field of nuclear physics. In particular, in the past two decades, the experimental synthesis of super-heavy elements (SHEs) [1–5] and theoretical studies on the production of SHEs have presented great challenges in the investigation of the heavy-ion reaction mechanism. Although there has been great progress in the study of the heavy-ion reaction mechanism and the related nuclear structures [6–21], the problems associated with the heavy-ion reactions and their mechanism remain unclear. The evolution of nuclear deformation is an important aspect of the nuclear reaction mechanism. The effects of deformations in heavy-ion reactions have been investigated preliminarily in Refs. [22–24]. In the dinuclear system (DNS) model, the deformation has been found to affect the interaction potential, the driving potential, the energy dissipation of the system, and the fusion cross sections [25–28]. In the reaction process, dynamical deformations of the two nuclei may appear [17], and thus, the static as well as dynamical deformations in the reaction process should be studied thoroughly. However, the dynamical deformations in the DNS model [17] are treated phenomenologically. Thus, the dynamical deformations in microscopical methods should be investigated further. More information, e.g., on the deformation for the calculations of interaction potential in DNS model, will be helpful for the development of the model. The dynamical quadrupole deformations evolved in an approaching process have been studied with the quantum molecular dynamics (QMD) model self-consistently [29]. In Ref. [27], it was found that the octupole deformations significantly affect the structure of driving potential. Thus, besides the quadrupole dynamical deformation, it is very important to investigate whether the dynamical octupole deformation exists in nuclei and its effects in heavy-ion reactions. Thus, in this letter, the dynamical octupole deformations for the projectile and target in the approaching process will be investigated with the QMD model. Further, because of the strong Coulomb interaction, the centers for protons and neutrons in a nucleus in the approaching process may separate from each other. Thus, the distributions for proton centers and neutron centers for four typical reaction channels are also discussed.

In the QMD model [30, 31], each nucleon is represented by a coherent state of a Gaussian wave packet,

$$\psi(\boldsymbol{r}) = \frac{1}{(2\pi\sigma_r^2)^{3/4}} \exp[-\frac{(\boldsymbol{r}-\boldsymbol{r}_i)}{(4\sigma_r^2)} + \frac{\mathrm{i}\boldsymbol{p}_i \cdot \boldsymbol{r}}{\hbar}] \quad (1)$$

where $\boldsymbol{r}_i$ and $\boldsymbol{p}_i$ are the centers of the i_{th} wave packet

in the coordinate and momentum space, respectively. σ_r denotes the widths of the wave packets. The one-body phase space distribution function for N distinguishable particles can be obtained by the Wigner transformation. The density distribution function of a system in coordinate space is given as

$$\rho(\boldsymbol{r}) = \sum_i \frac{1}{(2\pi\sigma_r^2)^{3/2}} \exp[-\frac{(\boldsymbol{r}-\boldsymbol{r}_i)^2}{(2\sigma_r^2)}] \quad (2)$$

In the QMD model, the nucleons in the system move in the self-consistently generated mean field. The time evolution of $\boldsymbol{r}_i$ and $\boldsymbol{p}_i$ is governed by Hamiltonian equations of motion:

$$\dot{\boldsymbol{r}}_i = \frac{\partial H}{\partial \boldsymbol{p}_i}, \quad (3)$$

and

$$\dot{\boldsymbol{p}}_i = -\frac{\partial H}{\partial \boldsymbol{r}_i}, \quad (4)$$

where H is the Hamiltonian and is expressed as

$$H = T + U_{\rm Loc} + U_{\rm Coul}, \quad (5)$$

where T, $U_{\rm Loc}$, and $U_{\rm Coul}$ represent the kinetic energy, nuclear local interaction potential energy, and Coulomb interaction potential energy, respectively. The positions for the nucleons of the projectile and target can be obtained by solving the Hamiltonian equations. Thus, the density distribution and the octupole moments for the system can be calculated. The nuclear octupole deformations can be estimated by the following relation [32]:

$$\beta_3 = [\sqrt{7\pi}/(3AR_0^3)]D, \quad (6)$$

where A, R_0, and D represent the mass number, equivalent radius, and octupole moment, respectively. The octupole moment at any time moment can be calculated as

$$D = \int_V \rho(2z^2 - 3x^2 - 3y^2) z {\rm d}\tau, \quad (7)$$

Figure 1 shows the dynamical octupole deformation parameters for four typical reaction channels with impact parameters $b = 0$ as a function of the distances between the mass centers for the projectile and target. The open and solid circles represent the deformation parameters for the projectile and the target, respectively. The positive direction of the Z-axis in the calculations is set as the direction from the projectile to the target. In Fig. 1(a), at an early stage of the collision, the projectile and target appear to be spherical. As they approach each other, the two nuclei are gradually distorted. When the central distance between two nuclei is about 12 fm, reflection asymmetric octupole deformations for both nuclei appear. The octupole deformations for the projectile and target increase as the central distance decreases, e.g., the octupole deformation parameters are about 0.15 when the central distance is about 11 fm. This phenomenon could be attributed to the strong long-range Coulomb potential. To lower the Coulomb potential, the projectile–target system adjusts its charge distribution, and a tip–tip orientation for the two octupole deformed nuclei can be observed. The developments of octupole deformations for the reactions ^{90}Zr +^{208} Pb, ^{91}Nb +^{238} U and ^{238}U +^{238} U are shown in Figs. 1(b), (c) and (d), respectively. For the symmetric projectile–target system shown in Fig. 1(a) and (d), the two fragments undergo the similar octupole deformations, whereas for the asymmetric projectile-target system shown in Fig. 1(b) and (c), the larger fragments undergo smaller octupole deformations and the smaller fragments undergo larger octupole deformations. This could be because it is easier for the light fragment to adjust its mass distribution, while this is difficult to achieve for the heavier fragment. With decreasing central distance, octupole deformation increases gradually. When the two fragments are very close to each other, the separation between the mass centers of the two heavy fragments remains almost constant, and the maximum octupole deformation may be obtained at this configuration, e.g., the maximum octupole deformation for ^{238}U +^{238} U at $E_{\rm c.m.}$ =880 MeV is about 0.2 at a central distance of about 13 fm. In DNS model [27], the octupole deformation plays an important role in the interaction potential and the driving potential. As reported in Ref. [27], the potential energy decreases by about 5 MeV due to the octupole deformation, and the structure of driving potential changes significantly. Owing to the dynamical octupole deformations shown in this letter, the calculation of the potential energy for a DNS configuration should be improved.

The dependence of the absolute values of maximum octupole deformation parameters on the incident energy for head-on collisions is shown in Fig. 2. As seen in Fig. 2(a), the maximum octupole deformations can reach about 0.6 at $E_{\rm c.m.}$=200 MeV. This implies that the projectile and target can get close enough and both undergo octupole deformations due to the effects of Coulomb repulsion between them. As the incident energy increases, there is less time for two fragments to adjust their deformations. When the incident energy is larger than 250 MeV, the octupole deformations are smaller than 0.2. In Figs. 2(b), (c), and (d), similar tendencies can be found. In Figs. 2(b) and (c), it is also seen that the light nucleus could obtain the larger maximum octupole deformation.

In some theoretical phenomenological models, the charges in nuclei are assumed to be uniformly dis-

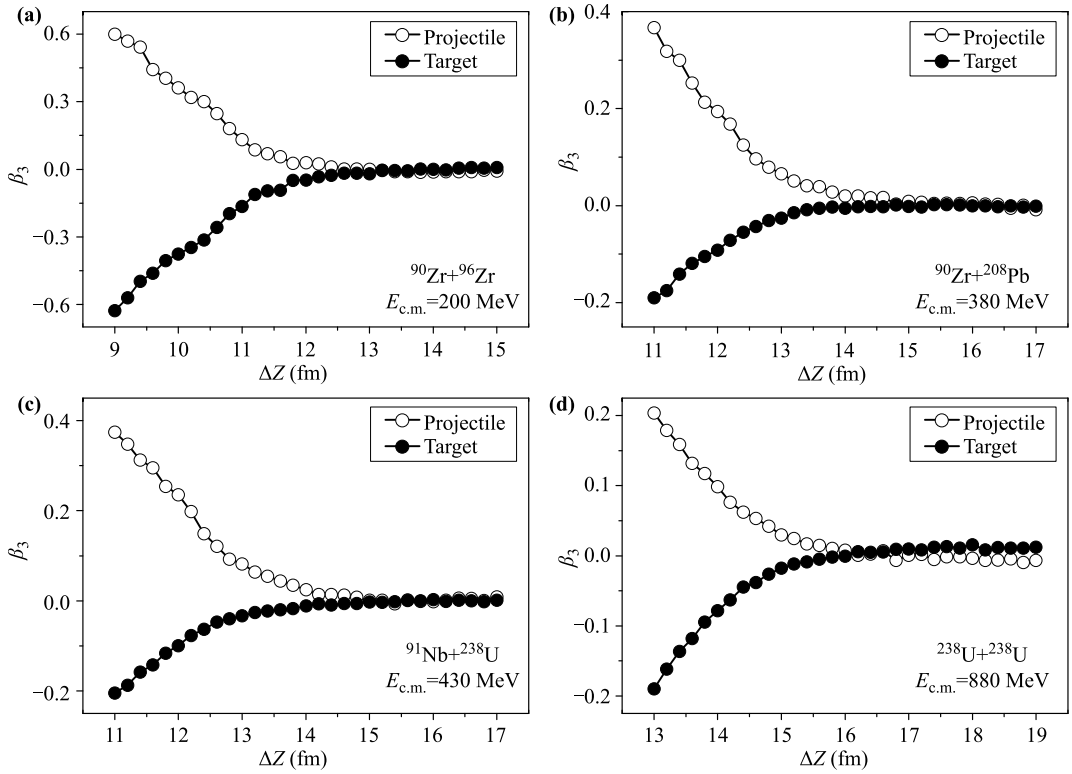

Fig. 1 Dynamical octupole deformations of projectile and target for **(a)** ^{90}Zr + ^{96}Zr, **(b)** ^{90}Zr + ^{208}Pb, **(c)** ^{91}Nb + ^{238}U, and **(d)** ^{238}U + ^{238}U as functions of the central distances between two nuclei.

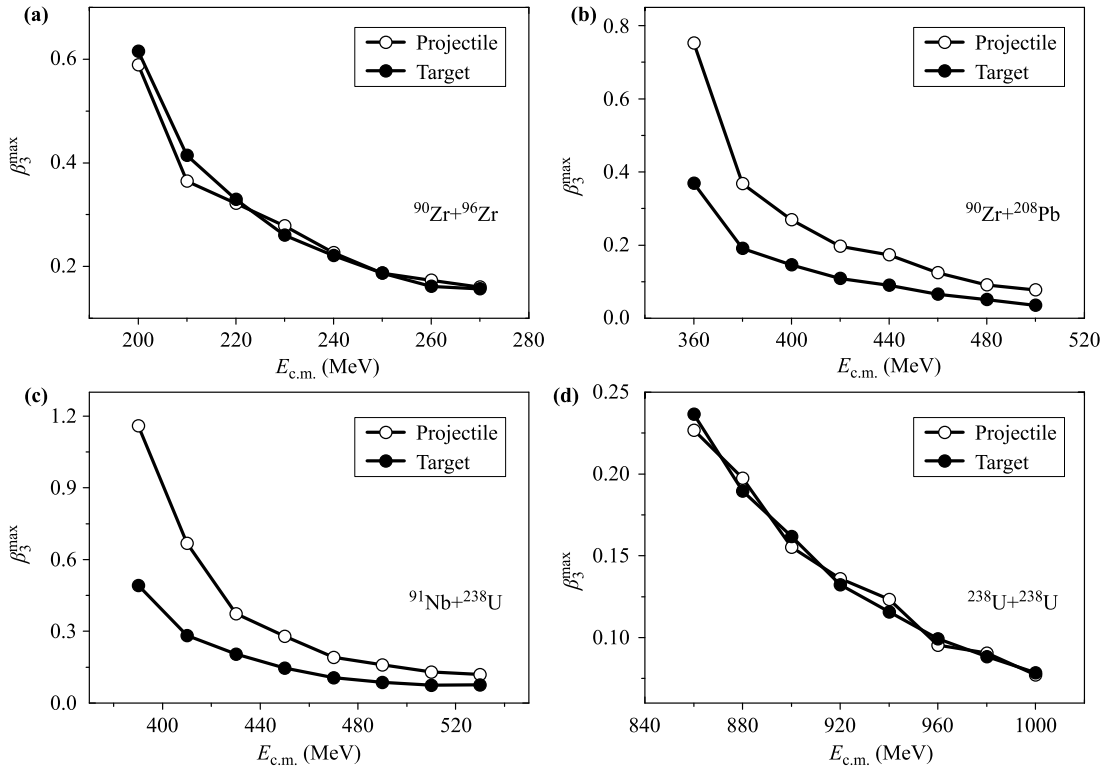

Fig. 2 The absolute values of maximum octupole deformation parameters for **(a)** ^{90}Zr + ^{96}Zr, **(b)** ^{90}Zr + ^{208}Pb, **(c)** ^{91}Nb + ^{238}U, and **(d)** ^{238}U + ^{238}U as a function of the incident energies.

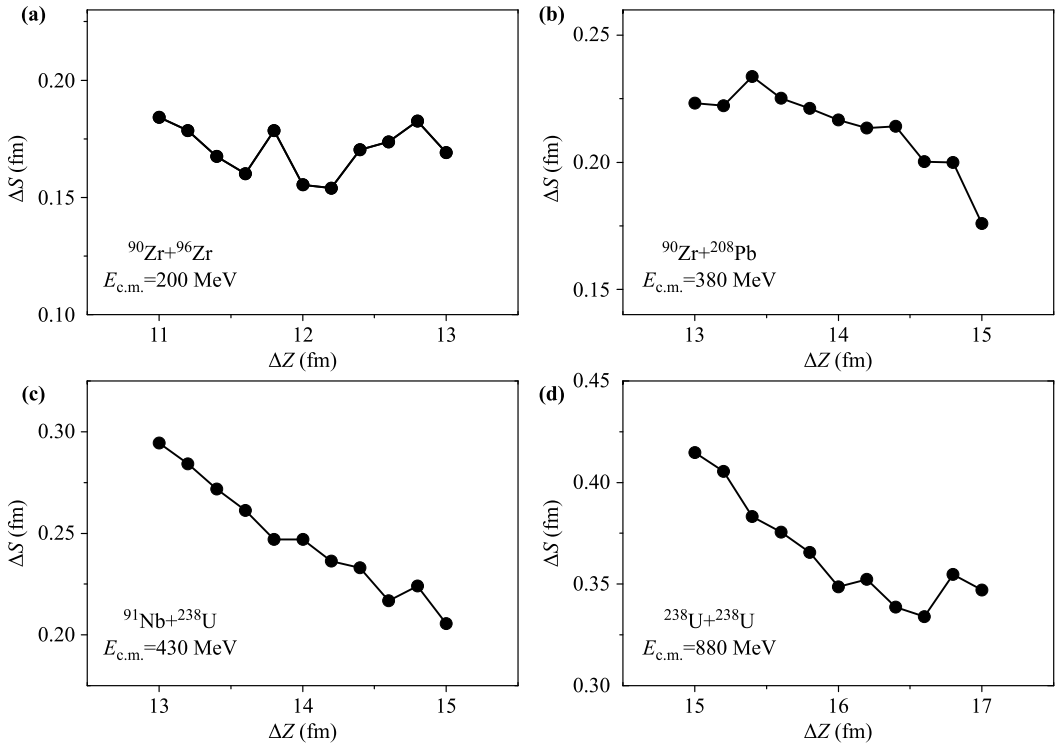

Fig. 3 Differences between separations for proton and neutron centers of two nuclei for incident channels **(a)** ^{90}Zr + ^{96}Zr, **(b)** ^{90}Zr + ^{208}Pb, **(c)** ^{91}Nb + ^{238}U, and **(d)** ^{238}U + ^{238}U versus the central distance between two nuclei.

tributed, and thus, the centers for protons and neutrons coincide. In this letter, the separation between the proton center of the projectile and that of the target $S_{\rm prot}$ and that for neutron centers $S_{\rm neut}$ are calculated, and the differences between them $\Delta S = S_{\rm prot} - S_{\rm neut}$ for four typical reaction channels with impact parameters $b = 0$ as a function of central distances are shown in Fig. 3. In Fig. 3(a), it can be seen that the separation between proton centers of two nuclei is about 0.16–0.18 fm larger than that for neutrons, which means that the centers for protons and neutrons deviate from each other due to the strong Coulomb potential. As the charge numbers for the projectile and target increase, the difference ΔS also increases. Further, from Figs. 3(b), (c), and (d), with decreasing distance between two nuclei, ΔS increases because of the larger Coulomb potential at shorter distances, e.g., in (d), at about 15 fm, ΔS is over 0.4 fm. These results imply that the effect of separation of proton and neutron centers should be considered while calculating the interaction potential between nuclei.

In summary, the dynamical octupole deformations developed in the approaching process for the heavy-ion reactions are studied with the QMD model. The results show that the octupole deformations of the two nuclei appear as they approach each other due to the strong Coulomb repulsion and decrease the total energy of the system. The dependence of the maximum octupole deformations on the incident energies for four typical reaction channels is also studied. The maximum octupole deformation increases as the incident energy decreases. The distributions for the proton and neutron centers of two nuclei during the approaching process are also studied. The separation between the proton centers for two nuclei is larger than that between neutron centers, owing to the strong Coulomb repulsion. The difference increases when the charge numbers for two fragments increase. Further, the difference also increases when two fragments get closer to each other. Further study is in progress.

Acknowledgements The work was supported by the National Natural Science Foundation of China (Grant Nos. 11475115, 10975100, 11275098, 10979066, and 11120101005), the National Basic Research Program of Ministry of Science and Technology of China (Grant No. 2007CB815000), the Knowledge Innovation Project of CAS (Grant Nos. KJCX2-EW-N01 and KJCX2-YW-N32). Part of the numerical results is obtained on the ScGrid of Supercomputing Center, CNIC of CAS.

References

1. S. Hofmann and G. Münzenberg, The discovery of the heaviest elements, *Rev. Mod. Phys.* 72(3), 733 (2000)
2. Y. T. Oganessian, V. K. Utyonkov, Y. V. Lobanov, F. S. Abdullin, A. N. Polyakov, I. V. Shirokovsky, Y. S. Tsyganov,

A. N. Mezentsev, S. Iliev, V. G. Subbotin, A. M. Sukhov, K. Subotic, O. V. Ivanov, A. N. Voinov, V. I. Zagrebaev, K. J. Moody, J. F. Wild, N. J. Stoyer, M. A. Stoyer, and R. W. Lougheed, Measurements of cross sections for the fusion-evaporation reactions $^{204;206;207;208}$Pb+ ^{48}Ca and ^{207}Pb+ ^{34}S: Decay properties of the even-even nuclides ^{238}Cf and ^{250}No, *Phys. Rev. C* 64(5), 054606 (2001)

3. Y. T. Oganessian, V. K. Utyonkov, Y. V. Lobanov, F. S. Abdullin, A. N. Polyakov, I. V. Shirokovsky, Y. S. Tsyganov, G. G. Gulbekian, S. L. Bogomolov, B. N. Gikal, A. N. Mezentsev, S. Iliev, V. G. Subbotin, A. M. Sukhov, A. A. Voinov, G. V. Buklanov, K. Subotic, V. I. Zagrebaev, M. G. Itkis, J. B. Patin, K. J. Moody, J. F. Wild, M. A. Stoyer, N. J. Stoyer, D. A. Shaughnessy, J. M. Kenneally, P. A. Wilk, R. W. Lougheed, R. I. Il'kaev, and S. P. Vesnovskii, Measurements of cross sections and decay properties of the isotopes of elements 112, 114, and 116 produced in the fusion reactions $^{233;238}$U, ^{242}Pu, and ^{248}Cm+^{48}Ca, *Phys. Rev. C* 70(6), 064609 (2004)
4. Y. T. Oganessian, V. K. Utyonkov, Y. V. Lobanov, F. S. Abdullin, A. N. Polyakov, R. N. Sagaidak, I. V. Shirokovsky, Y. S. Tsyganov, A. A. Voinov, G. G. Gulbekian, S. L. Bogomolov, B. N. Gikal, A. N. Mezentsev, S. Iliev, V. G. Subbotin, A. M. Sukhov, K. Subotic, V. I. Zagrebaev, G. K. Vostokin, M. G. Itkis, K. J. Moody, J. B. Patin, D. A. Shaughnessy, M. A. Stoyer, N. J. Stoyer, P. A. Wilk, J. M. Kenneally, J. H. Landrum, J. F. Wild, and R. W. Lougheed, Synthesis of the isotopes of elements 118 and 116 in the ^{249}Cf and ^{245}Cm +^{48}Ca fusion reactions, *Phys. Rev. C* 74(4), 044602 (2006)
5. Z. Y. Zhang, Z. G. Gan, L. Ma, M. H. Huang, T. H. Huang, X. L. Wu, G. B. Jia, G. S. Li, L. Yu, Z. Z. Ren, S. G. Zhou, Y. H. Zhang, X. H. Zhou, H. S. Xu, H. Q. Zhang, G. Q. Xiao, and W. L. Zhan, Observation of the superheavy nuclide ^{271}Ds, *Chin. Phys. Lett.* 29(1), 012502 (2012)
6. G. Adamian, N. Antonenko, and W. Scheid, Model of competition between fusion and quasifission in reactions with heavy nuclei, *Nucl. Phys. A* 618(1–2), 176 (1997)
7. G. Mandaglio, G. Giardina, A. K. Nasirov, and A. Sobiczewski, Investigation of the ^{48}Ca+ $^{249-252}$Cf reactions synthesizing isotopes of the superheavy element 118, *Phys. Rev. C* 86(6), 064607 (2012)
8. V. I. Zagrebaev, Y. Aritomo, M. G. Itkis, Y. T. Oganessian, and M. Ohta, Synthesis of superheavy nuclei: How accurately can we describe it and calculate the cross sections? *Phys. Rev. C* 65(1), 014607 (2001)
9. Z. H. Liu and J. D. Bao, Synthesis of superheavy element 120 via ^{50}Ti+^{A}Cf hot fusion reactions, *Phys. Rev. C* 80(5), 054608 (2009)
10. G. F. Dai, L. Guo, E. G. Zhao, and S. G. Zhou, Effect of tensor force on dissipation dynamics in timedependent Hartree-Fock theory, *Sci. China-Phys. Mech. Astron.* 57(9), 1618 (2014)
11. C. Shen, G. Kosenko, and Y. Abe, Two-step model of fusion for the synthesis of superheavy elements, *Phys. Rev. C Nucl. Phys.* 66(6), 061602(R) (2002)
12. J. J. Shen and C. W. Shen, Theoretical analysis of mass distribution of quasifission for ^{238}U-induced reactions, *Sci. China-Phys. Mech. Astron.* 57(3), 453 (2014)
13. Z. G. Gan, X. H. Zhou, M. H. Huang, Z. Q. Feng, and J. Q. Li, Predictions of synthesizing element 119 and 120., *Sci. China-Phys. Mech. Astron.* 54(S1 Supp.1), s61 (2011)
14. Z. Q. Feng, G. M. Jin, F. Fu, and J. Q. Li, Production cross sections of superheavy nuclei based on dinuclear system model, *Nucl. Phys. A* 771, 50 (2006)
15. K. P. Xie, W. Y. Ke, W. Y. Liang, X. M. Fu, C. F. Jiao, J. C. Pei, and F. R. Xu, Collective rotations of fission isomers in actinide nuclei, *Sci. China-Phys. Mech. Astron.* 57(2), 189 (2014)
16. N. Wang, E. G. Zhao, and W. Scheid, Synthesis of superheavy nuclei with $Z = 118$ in hot fusion reactions, *Phys. Rev. C* 89(3), 037601 (2014)
17. N. Wang, E. G. Zhao, W. Scheid, and S. G. Zhou, Theoretical study of the synthesis of superheavy nuclei with $Z = 119$ and 120 in heavy-ion reactions with trans-uranium targets., *Phys. Rev. C* 85(4), 041601(R) (2012)
18. J. Xu, B. A. Li, W. Q. Shen, and Y. Xia, Dynamical effects of spin-dependent interactions in low- and intermediate-energy heavy-ion reactions, *Front. Phys.* 10, 102501 (2015)
19. H. L. Liu and F. R. Xu, Calculations of electric quadrupole moments and charge radii for high-K isomers, *Sci. China-Phys. Mech. Astron.* 56(11), 2037 (2013)
20. L. W. Chen, C. M. Ko, B. A. Li, and G. C. Yong, Probing the nuclear symmetry energy with heavy-ion reactions induced by neutron-rich nuclei, *Front. Phys.* 2(3), 357 (2007)
21. A. M. Zhao, W. M. Sun, and H. S. Zong, Influence of thermalization on the initial condition for heavy ion collisions, *Sci. China-Phys. Mech. Astron.* 57(11), 2060 (2014)
22. G. Wolschin and W. Noerenberg, Analysis of relaxation phenomena in heavy-ion collisions, *Z. Phys. A: Hadrons Nucl* 284, 209 (1978)
23. A. S. Jensen and C. Y. Wong, Coulomb distortion in heavy-ion reactions, *Phys. Rev. C* 1(4), 1321 (1970)
24. S. K. Samaddar, M. I. Sobel, J. N. De, S. I. A. Garpman, D. Sperber, M. Zielinska-Pfabe, and S. Møller, A classical dynamical model with shape deformation for strongly damped collisions, *Nucl. Phys. A* 332(1–2), 210 (1979)
25. Q. F. Li, W. Zuo, W. F. Li, N. Wang, E. Zhao, J. Li, and W. Scheid, Deformation and orientation effects in the driving potential of the dinuclear mode, *Eur. Phys. J. A* 24(2), 223 (2005)
26. W. Li, N. Wang, F. Jia, H. Xu, W. Zuo, Q. Li, E. Zhao, J. Li, and W. Scheid Particle transfer and fusion cross-section for super-heavy nuclei in dinuclear system, *J. Phys. G* 32(8), 1143 (2006)
27. N. Wang, E. G. Zhao, W. Scheid, and S. G. Zhou, Influence of octipole deformation and orientation on the potential en-

ergy surface in the di-nuclear system model, *Chin. Phys. C* 34(10), 1615 (2010)

28. N. Wang, L. Dou, E. G. Zhao, and W. Scheid, Nuclear hexadecapole deformation effects on the production of superheavy elements, *Chin. Phys. Lett.* 27(6), 062502 (2010)
29. L. Dou, N. Wang, and E. G. Zhao, Nuclear dynamical quadrupole deformations in heavy-ion reactions, *Chin. Phys. Lett.* 28(12), 122401 (2011)
30. J. Aichelin, Quantum molecular dynamicsa dynamical microscopic n-body approach to investigate fragment formation and the nuclear equation of state in heavy ion collisions, *Phys. Rep.* 202(5–6), 233 (1991)
31. N. Wang, X. Z. Wu, and Z. X. Li, Dynamic study of fusion reactions for $^{40;48}$Ca+ $^{90;96}$Zr around the Coulomb barrier, *Phys. Rev. C* 67(2), 024604 (2003)
32. X. T. Lu, D. X. Jiang, and Y. L. Ye, Nuclear Physics, Beijing: Atomic Energy Publishing House, 2000